ELSEVIER

Journal of Chromatography A, 953 (2002) 151–163

JOURNAL OF CHROMATOGRAPHY A

www.elsevier.com/locate/chroma

Effects of solvent density on retention in gas–liquid chromatography
I. Alkanes solutes in polyethylene glycol stationary phases

F.R. González[a,b,*], J. Pérez-Parajón[a], J.A. García-Domínguez[a]

[a]*Instituto de Química-Física Rocasolano, CSIC, Serrano 119, 28006 Madrid, Spain*

[b]*Div. Química Analítica, Fac. de Ciencias Exactas, Universidad Nacional de La Plata, 47 y 115, 1900 La Plata, Argentina*

Received 14 December 2001; received in revised form 8 February 2002; accepted 8 February 2002

Abstract

Gas–liquid chromatographic columns were prepared coating silica capillaries with poly(oxyethylene) polymers of different molecular mass distributions, in the range of low number-average molar masses, where the density still varies significantly. A novel, high-temperature, rapid evaporation method was developed and applied to the static coating of the low-molecular-mass stationary phases. The analysis of alkanes retention data from these columns reveals that the dependence of the partition coefficient with the solvent macroscopic density is mainly due to a variation of entropy. Enthalpies of solute transfer contribute poorly to the observed variations of retention. Since the alkanes solubility diminishes with the increasing solvent density, and this variation is weakly dependent with temperature, it is concluded that the decrease of free-volume in the liquid is responsible for this behavior. © 2002 Published by Elsevier Science B.V.

Keywords: Density; Partition coefficients; Stationary phases, GC; Gas chromatography; Thermodynamic parameters; Alkanes; Poly(ethylene glycol)

1. Introduction

The way particles arrange in a solvating medium determines its density. So, in principle, there will be several molecular aspects of solvation linked to density, e.g., the solvent free-volume and the distribution of solvent particles in the surroundings of a solute molecule (the radial distribution function). The understanding of the solvent density influence upon solvation properties of different solutes undoubtedly has importance from practical and theoretical viewpoints. For example, to elucidate if polymers having the same chemical composition, but not the same density, different stationary phases should be considered, or if otherwise the retention information from one can be applied to the others by making simple corrections, has relevant practical implications for gas–liquid chromatography (GLC).

In order to make feasible further theoretical developments, Prigogine [1] proposed that the degrees of freedom of a molecule could be divided into those that are affected by the density of its environment and those that are insensible to this density. The idea is generally accepted that only low frequency motions of the molecules are affected by the density of their environment [2]. This has led to the hypothesis

*Corresponding author. Instituto de Química-Física Rocasolano, CSIC, Serrano 119, 28006 Madrid, Spain.

E-mail address: rex@quimica.unlp.edu.ar (F.R. González).

0021-9673/02/$ – see front matter
PII: S0021-9673(02)00162-0

that, mostly, the internal degrees of freedom of a solute should not be affected by a gas–liquid transfer process [3]. Notwithstanding, there is no abundance of direct experimental information which indicates ranges of frequencies where these basic hypotheses are applicable. Capillary gas chromatography is potentially useful as a technique for studying heat capacity differences of solute transfer in discrete temperature intervals, and then it is capable of providing important information on this issue [4]. In a feedback, the resultant knowledge from such investigations could help to answer questions of practical nature for chromatography itself.

Through the performance of Monte Carlo molecular simulations, Martin et al. [5] concluded that the decrease observed experimentally for methane's partition coefficient K [6], on the increasing chain length of *n*-alkanes solvents, is due to the increment of density along the homologous series. This variation would affect the environment of the solute principally through repulsive forces, as the solvent density increases. This is a behavior naturally expected when the partition coefficient of the solute is $K<1$ [7–9], as in the case of the cited system, because the solvation process is mainly controlled by the free volume in the solvent. Despite its practical and theoretical importance, specific studies on the effects of the solvent density on K are lacking for solutes with $K>1$.

Polymer crosslinking is currently applied in the manufacture of wall-coated capillary columns. This process modifies the density of the original stationary phase, generally increasing it, introduces new chemical groups and also modifies the physical properties of the polymer strands, imposing restrictions to the possible configurations they can adopt around a solute molecule. The crosslinking reaction is conducted in situ after the capillary has been coated [10], consequently, the control of the stationary phase's final density is unfeasible. The behavior of crosslinked stationary phases has been compared with the unmodified ones by contrasting relative retention parameters and retention factors [11–13]. However, the effect of crosslinking upon absolute values of K has not been studied thoroughly from a thermodynamic standpoint. Only such an approach would admit understanding cause–effect relationships, because the simultaneous variation of the solvation properties of the reference screens out the effects on the studied solute, if relative parameters are utilized.

The aim of this work is to study the influence of the macroscopic density of poly(oxyethylene) stationary phases, ρ_L, on the chromatographic retention of *n*-alkane solutes. The polymers employed in this study have different number-average molecular masses, $\bar{M}_n$ [14], in the range of low $\bar{M}_n$, where the asymptotic region of the function $\rho_L(\bar{M}_n)$ has not been reached yet. They also have different molecular mass distributions (MWDs). In two cases the polydispersity of the stationary phase was incremented artificially by preparing blends with two polymers of different $\bar{M}_n$. In principle, the modification of the MWD in oligomers not only can affect the retention through the variation of density, but also through the variation of end-groups concentration. Further comparisons of partition coefficients with crosslinked stationary phases were carried out.

Schweitzer and Staudinger initiated the research on the synthesis of poly(oxyethylene) through the alkali-catalyzed polymerization of ethyleneoxide [15,16]. The trivial name polyethylene glycol (PEG) designating these polymers derives from the assumption that the reaction, carried out employing aqueous alkali solutions, is a polycondensation where ethyleneglycol (which forms first) progressively adds more ethyleneoxide molecules [16]. Since this process includes water, hydrates with end –OH groups are invariably formed [15–19] (see Appendix A). After the reaction is stopped, the alkali is neutralized using hydrochloric or acetic acids, and the water eliminated through vacuum evaporation. Oligomers or low-molecular-mass polymers are obtained in this way, usually with $\bar{M}_n<10^4$. $\bar{M}_n$ is determined currently through end-group analysis, by the homologous conversion of the hydrates to diacetates. This value of $\bar{M}_n$ is utilized as a commercial designation for the low-molecular-mass polymers: e.g., Carbowax 1000 of Union Carbide [20]. The synthesis of high-molecular-mass PEG, up to $\bar{M}_n$ in the order of 10^6, is feasible through the catalysis with alkaline earth carbonates [21] and Al organic catalysts [22]. An important aspect that must be taken into consideration, is that the high-molecular-mass polymers ($\bar{M}_n>10^4$) differ in their physical properties with the oligomers. A very important manifestation of these

differences takes place in the IR spectra [23]. For the high $\bar{M}_n$ compounds, a C–O–C bending band splits into two components, at $\tilde{\nu}=527$ and 507 cm^{-1}, and a new band appears at low $\tilde{\nu}$. As will be shown here, the thermal expansion coefficient α_L differs considerably.

PEG has hydrophilic and lipophilic characters, and is generally lyophilic [16]. Water is a remarkable good solvent, and the solubility in some organic solvents, such as dichloromethane and chloroform, is explainable since PEGs are polyethers. Nonetheless, ethers are poor solvents.

The influence of the PEG $\bar{M}_n$ on some retention parameters, such as the retention factor *k*, the specific retention volume V_g and the Kovats index *I*, has been investigated experimentally for different types of solutes [24–26]. By using packed columns of the same dimensions and nearly the same amount of liquid loading, it was found that there is a strong variation of *k* for the low-$\bar{M}_n$ stationary phases, while an asymptotic behavior is reached for the high-$\bar{M}_n$ ones [24]. This evolution, towards an asymptotic behavior at increasing $\bar{M}_n$, is a generalized feature observed in many other physical polymer properties [27]. There have also been attempts to explain the effect of the stationary phase molecular mass on the activity coefficients of different solutes through some theoretical and semiempirical arguments [28,29].

In non-electrolyte solutions the solute–solvent interactions involve a short range of distances. Only solvent particles that are at distances not much farther than 10 Å contribute significantly to the force field exerted on the solute [30]. Therefore, the chain length of the polymeric solvent, as measured by $\bar{M}_n$, has not a direct causality on the solvation behavior of a small solute. Its effect is rather indirect, since the MWD and the structural characteristics of the polymer chain, such as its rigidity and the polymer–polymer interactions (intra- and intermolecular interactions), determine the final density and distribution of particles in the solvating medium. From the perspective of molecular thermodynamics, one of the solvent properties that primarily control the solubility is the numeral density of particles [2,3,31]. This density has a very complex relationship with the molecular mass, even for monodisperse polymers, and presently there are no theories capable of deriving general explicit relationships between them. In view of these facts, the primary variable utilized in this work to correlate and study the retentive properties of the polymers is not an average of the molecular mass as $\bar{M}_n$.

2. Experimental

2.1. Materials

The polymers employed in this work for coating the silica capillaries are indicated in the first column of Table 1. These are Carbowax (CW) 600, 1000, 1540, M1 and M2. The latter two are polymer blends prepared by mixing liquid CW 600 and 1000 with mass-fractions of 0.7039–0.2961 and 0.3143–0.6857, respectively. In the second column of Table 1 are shown the values of $\bar{M}_n$ for the blends

Table 1
Specifications of the employed stationary phases and columns

Stationary phase denomination	PEG nominal $\bar{M}_n$	Number-average degree of polymerization, $\bar{n}_n$	PEG density regression parameters, $\alpha_L \cdot 10^4$ (K^{-1}); *b*	Concentration of coating solutions, C_o (g/ml)	Column phase ratio, β, at 80 °C
Carbowax 600	600	13	7.908; 0.1889	0.00900	125
M1	681	15	7.800; 0.1803	0.00897	124
M2	827	18	7.632; 0.1610	0.00900	122
Carbowax 1000	1000	22	7.688; 0.1509	0.00908	119
Carbowax 1540	1500	34	7.847; 0.1407	0.00898	119

Polymers M1 and M2 are blends obtained by mixing liquid Carbowax 600 and 1000, respectively, with mass fractions: (0.7039–0.2961) and (0.3143–0.6857). The equation describing the PEG density is: $\ln \rho_L = b - \alpha_L T$, where *T* was expressed in °C, and ρ_L in g/ml, so the units and significance of *b* correspond to these conditions. The number-average degree of polymerization was calculated according to Eq. (A.6) and the phase ratio according to Eq. (3).

calculated from the nominal values of their components according to (see Appendix A):

$$\bar{M}_n = \left(\frac{\omega_A}{\bar{M}_{nA}} + \frac{\omega_B}{\bar{M}_{nB}} \right)^{-1} \quad (1)$$

$\bar{M}_{nA}$, $\bar{M}_{nB}$, ω_A and ω_B are the number-average molecular masses and mass fractions of the components in the mixture. In the third column of Table 1 are shown the number-average degrees of polymerization, $\bar{n}_n$, i.e., the number of structural units corresponding to $\bar{M}_n$ (see Appendix A).

The Carbowaxes were those fractionated and commercialized by Altech (USA). Prior to their use, the pH was checked in order to avoid any remains of the acids employed by the manufacturer in the post-reaction neutralization. In the case of CW 600, presence of acetic acid was detected. This was esterified, and the ester eliminated through vacuum evaporation. All polymers were first dried under vacuum at 80 °C, taking into account their great affinity to water.

Densities of the liquid polymers at $T > 70$ °C were determined by pycnometry. The experimentally measured temperature dependence of densities is shown in Fig. 1. The numerical values of the parameters, corresponding to a linear regression of ln ρ_L vs. T, are tabulated in the fourth column of Table 1. This representation implies assuming a constant thermal expansion coefficient α, which is a usual thermodynamic approximation when there are no transitions:

$$\alpha \equiv \frac{1}{V} \cdot \frac{dV}{dT} = \frac{-d\ln \rho}{dT} \quad (2)$$

Considering the experimental conditions, the indication for a constant pressure and composition in Eq. (2) was omitted, so the partial derivatives were replaced by total derivatives. All the employed low-molecular-mass polymers yield similar thermal expansion coefficients, with an average of $\alpha_L = 7.8 \cdot 10^{-4}$ K^{-1}. This differs considerably with those values measured by Kersten et al. for Carbowax 20M [32] and measured in this work for Superox 20M. These are significantly higher: $\alpha_L = 9.5 \cdot 10^{-4}$ and $9.3 \cdot 10^{-4}$ K^{-1}, respectively. It must be remarked that $\bar{M}_n = 20 \cdot 10^3$ belongs to the asymptotic region of functions $k(\bar{M}_n)$ and $\rho_L(\bar{M}_n)$. Plots of k versus $\bar{M}_n$ can be seen in Ref. [24], and the latter function is shown in Fig. 2.

Contrary to what is most usual for vinyl polymers with flexible backbones, the density of PEG oligo-

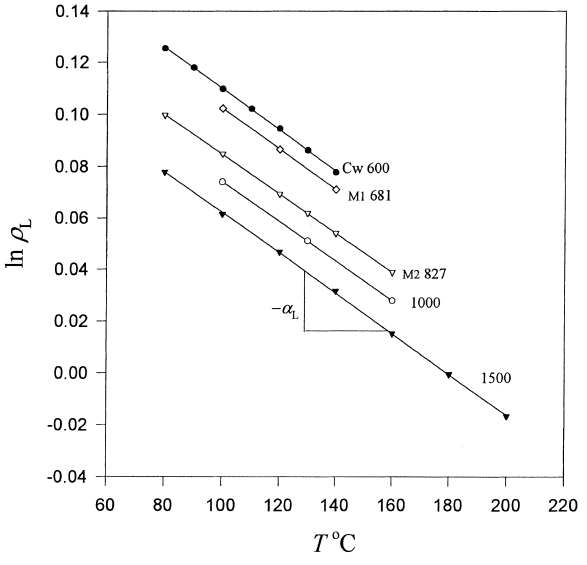

Fig. 1. Dependence of the stationary phase density with temperature. The thermal expansion, α_L, is constant in the chromatographic interval.

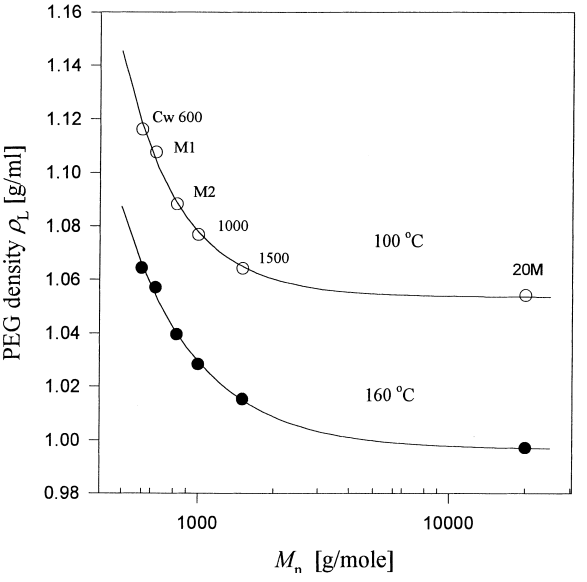

Fig. 2. Variation of the PEG density with the number-average molecular mass, $\bar{M}_n$, for two temperatures.

mers decreases by increasing $\bar{M}_n$. This is a notable characteristic of these substances to which little attention has been paid.

The employed silica capillaries were from MicroQuartz (Germany) and belong to the same coil with a bore diameter of 250 μm, with an –OH group content between 100 and 500 ppm. By request, the thermal expansion was measured by the manufacturer. The reported average coefficient is $\alpha_{SiO_2} = 1.957 \cdot 10^{-6}\ K^{-1}$.

2.2. Columns

The columns were prepared by applying the static method [10], so the phase ratio β can be known accurately. This can be calculated at any temperature without the explicit knowledge of the geometric parameters of the column, by making no approximation other than assuming in the chromatographic range a constant thermal expansion of the silica wall, α_{SiO_2}. The derived expression is (see Appendix B):

$$\beta(T) = \frac{\rho_L(T)}{C_o} \cdot e^{\alpha_{SiO_2}(T-T_o)} - 1 \quad (3)$$

C_o is the concentration of the stationary phase solution employed for filling the capillary at the ambient temperature T_o. In general, β can be determined with four significant digits, if an adequate amount of coating solution is prepared. In our particular case, the coating solution was prepared in a small 10.00±0.02 ml tapered flask, first weighing the polymer as liquid, previous homogenization, and then taking to volume with the solvent. With the amount of polymer weighted, we can only report three significant digits for β. The values of C_o and β are reported, respectively, in the fifth and sixth columns of Table 1.

The solvents employed for preparing the coating solutions were absolute ethanol for CW 600, 1000, M1 and M2, and a mixture of dichloromethane-ethanol (1:9, v/v) for CW 1540. Ethanol has the advantage of a low contact angle with silica, but it is not a good solvent for the higher-$\bar{M}_n$ compounds. Dichloromethane is a better solvent, but has the disadvantages of not wetting well the capillary, invariably has small traces of heavy metals and is chemically unstable. At high temperatures free radicals can promote undesired reactions in the stationary phase. Water was not used due to the excessively high evaporation temperatures required, which are incompatible with the employed polymers.

A high-temperature column evaporation method was developed, designing a special oven for this purpose. Details will be given elsewhere (patent pending). The advantages of this method are that it reduces the evaporation time from days, for the current vacuum procedure [33], to hours, and that at increasing temperatures the contact angle of the solvent is diminished. A wider spectrum of possibilities is thus opened for the selection of the employed solvents.

The evaporation was carried out at a column rate of 6.6 m/h, at 210 °C, controlling the process visually. All columns were 30 m long, taking 4.5 h to evaporate. Immediately after the evaporation finished, the closed end of the column was cut-off and an N_2 flow connected, ensuring that the temperature remained constant. Twenty minutes after the gas flow was connected, the temperature was reduced to 160 °C, and the column was left overnight in this condition. The next day the column was cooled down, the gas flow disconnected, and it was transferred to a HP 5890 Series II gas chromatograph (USA). Prior to starting the chromatographic run, the columns were conditioned at 220 °C for approximately 2 h, until low signals and stable baselines were attained.

2.3. Chromatographic measurement

Our purpose is to study the effect of the PEG density on the solubility of *n*-alkanes, then *K* should be determined. Although partition is known to be the most important contribution to retention in the studied system, certain incidence of interfacial effects is expected [9,34–37]. In order to minimize these effects, all columns were prepared with the same ratio of liquid volume to interfacial area, i.e., the same film thickness: $d_f = V_L/A_i = 0.5$ μm. This value is a compromise between the thickest film possible, with a high column efficiency. All runs were made over 80 °C. In these conditions it is expected that *K* will be the major contribution to the apparent coefficient K_{ap}. The latter also accounts for the contributions of interfacial excesses, and then it

depends on d_f, but is easily calculable from the raw experimental retention data of a single column [9]:

$$K_{ap} = k\beta = [(t_R/t_M) - 1]\beta \quad (4)$$

where t_R is the retention time. The gas hold-up t_M was determined as in Ref. [9]. For simplicity, all reported values of K_{ap} will be indicated as K.

The solutes were injected as vapors by applying the ''wet-needle'' technique, employing split ratios greater than 100:1. Progressively, the injected quantities were diminished until important variations of peak areas only affected the last digit of t_R, and these data were considered only.

3. Results

3.1. Correlation of alkanes solubility with PEG densities

We shall compare firstly our results with the precedents from the literature. Therefore, analyzing the behavior of retention with the PEG molecular mass is unavoidable, since this has been the variable currently utilized. Fig. 3 illustrates, in the example of *n*-dodecane, the behavior of ln K with $\bar{M}_n$. We have included data measured by Poole et al. in packed columns of Carbowax 20M [34]. A similar behavior is observed by representing K instead of its logarithm. These results are consistent with the observations of k made by Taleb-Bendiab and Vergnaud [24] on packed columns. The asymptotic behavior is similar to that of function $\rho_L(\bar{M}_n)$ in Fig. 2, with the opposite trend but following the same mathematical form (filled lines in the figures).

Since from a molecular viewpoint the numeral density of solvent particles is a primary variable governing the solvation of a solute, the first question arising is which particles can we consider? In the case of PEG oligomers, should they be atoms, monomers, or molecules? If molecular domains remain segregated, due to the predominance of folded molecular conformations, then the density of molecules would be an appropriate variable for correlating a process mainly controlled by the solvent free-volume. The reason is that in this case the excluded volume is defined by the volume pervaded

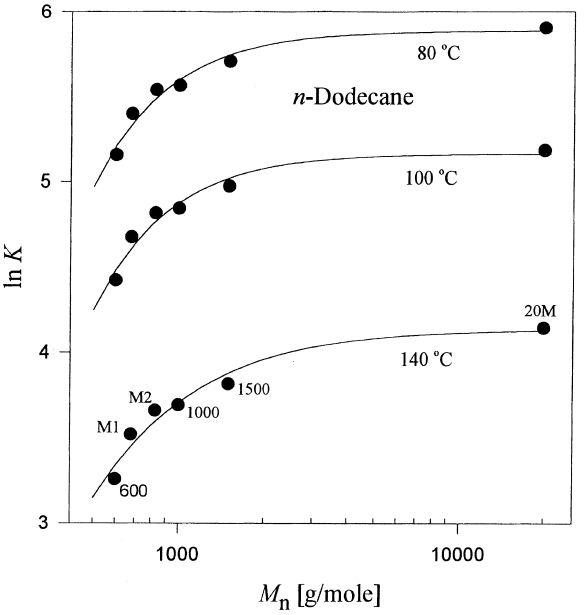

Fig. 3. Behavior of ln K with the number-average molecular mass $\bar{M}_n$, for *n*-dodecane at three different temperatures. The trend is opposite to Fig. 2 but resembles its asymptotic behavior.

by the segregated molecules and not by individual monomers. On the contrary, if molecular domains are deeply interpenetrated, then, the density of monomers or atoms would be a more appropriate choice. In an attempt to enlighten this issue, we could plot K versus the density corresponding to each case and analyze the nature of the correlation.

The solvent density reveals the average mass of atoms per unit volume in the liquid, and is our most basic and accessible variable. Fig. 4 illustrates the behavior of K as function of the stationary phase density for a given solute. The observed behavior is nearly the same in a wide interval of temperature, and similar for different homologues, as illustrated in Fig. 5. In a first approach, one would be tempted to assimilate empirically these behaviors to a linear function such as those linear regressions depicted for the upper curves, assuming that the dispersion of data is due to the experimental error. In that case it should be admitted that the stationary phases having broad MWDs (M1 and M2) practically behave as the others. Fig. 6 shows the correlation found with the numeral density of molecules, ρ_M, calculated according to Eq. (A.8) (see Appendix A). Fig. 7 reveals that

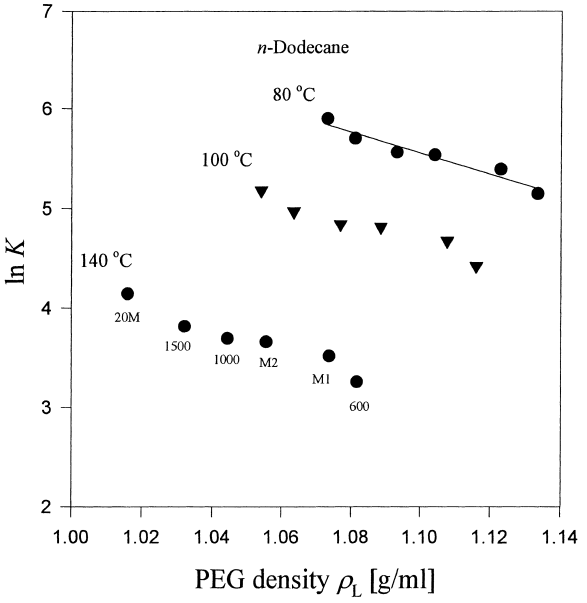

Fig. 4. Behavior of ln K with the stationary phase density for n-dodecane at different temperatures.

there is a much more complex behavior with the numeral density of monomers, ρ_m. It must be pointed out that the variation of ρ_m, with the PEG's chain

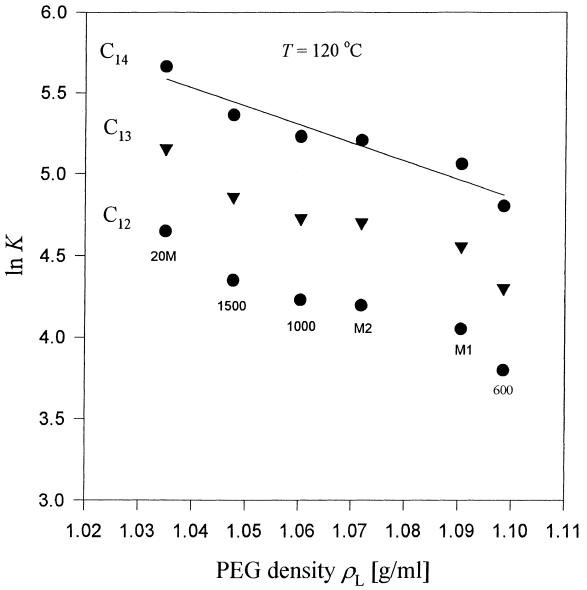

Fig. 5. Behavior of ln K with the stationary phase density for three different n-alkanes at 120 °C.

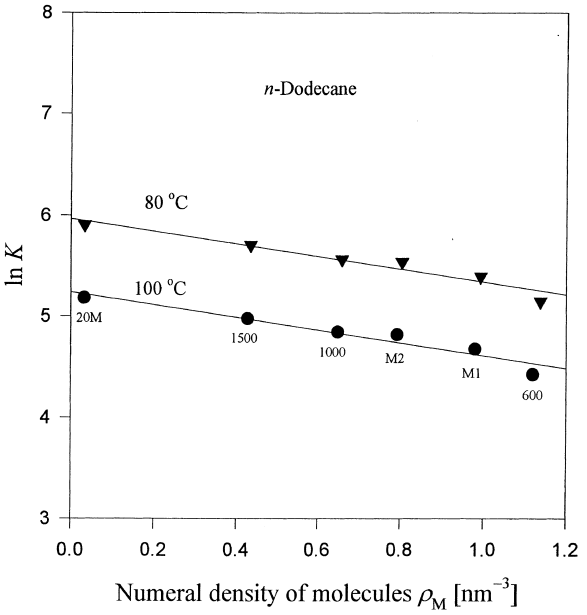

Fig. 6. Variation of ln K for n-dodecane with the numeral density of solvent molecules, ρ_M, at 80 °C and 100 °C. The density is expressed as the average number of molecules per nm^3.

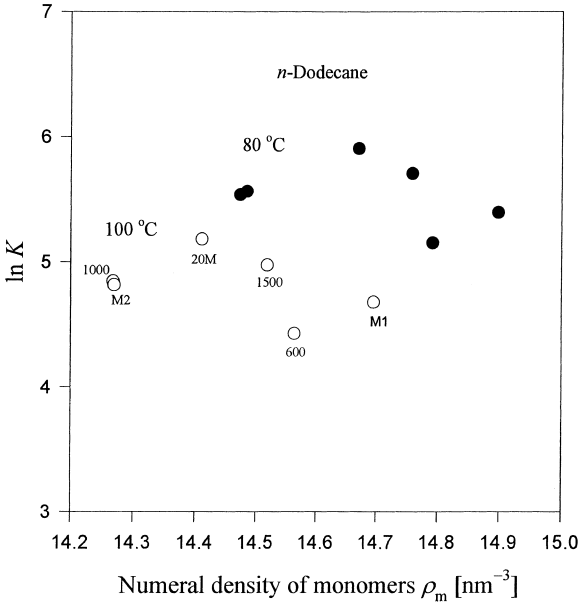

Fig. 7. Variation of ln K of n-dodecane with the numeral density of solvent monomers ρ_m at 80 °C and 100 °C. The density is expressed as the average number of monomers per nm^3.

length, is extremely small as compared, for example, with the variations in *n*-alkanes solvents having similar number of monomers [5].

3.2. Thermodynamic effects by variations of the PEG density

Determination of K as function of T was carried out for all the columns. These data were utilized for obtaining the enthalpy and entropy of solute transfer, ΔH^* and ΔS^* (the asterisk indicates that the thermodynamic functions correspond to the process of transferring one solute molecule from the ideal gas to a fixed position in the liquid [3,4]). The functions were obtained at each temperature calculating numerically the first derivative of ln $K(T)$ in accordance with Ref. [4]. Since the intervals of T for the $K(T)$ data were 20 °C, no analysis for the heat capacity of transfer is pretended here. Fig. 8 illustrates the results using the example of *n*-tridecane, comparing ΔH^* and ΔS^* for CW 600 and 1000. It is seen that the effect on the alkane solubility exerted by the increase of density, when changing phases from CW 1000 to 600, is principally due to a variation in the entropy of the solute transfer process. The change (CW 1000→600) increases the negative entropic contribution to ln K, and thus contributes to diminish the solubility. On the contrary, the enthalpic term contributes to increase the solubility as the density increases. Since, in the case of tridecane, the entropic effect is three times greater than the enthalpic, the net effect is a reduction of K by increasing the density. The impact of the entropic effect increases when the chain length of the alkane is shortened, as indicated in Table 2. For the lower homologues, the entropy change accounts for the most important part of the observed differences in K, which originates in the variations of density.

Another important issue revealed by Fig. 8 is that no major changes in the shapes of $\Delta H^*(T)$ and $\Delta S^*(T)$ occur within the applied variations of density. An almost parallel curve shift takes place in the cases of C_{10} to C_{14}.

3.3. Thermodynamic effects by PEG crosslinking

We shall compare here the behavior of crosslinked PEG stationary phases with the unmodified ones studied in this work. Following the preceding results, we can formulate an immediate question about the influence of PEG crosslinking on retention. Which effect will predominate? Will it be the mainly entropic simple one, resulting from an increase of density, or we should expect a complex enthalpic–entropic effect originated in the introduction of the vinyl chain-linkages?

In Fig. 9 we perform the same thermodynamic comparison, as in Section 3.2, for the commercial crosslinked phases AT-wax and HP-Innowax. The

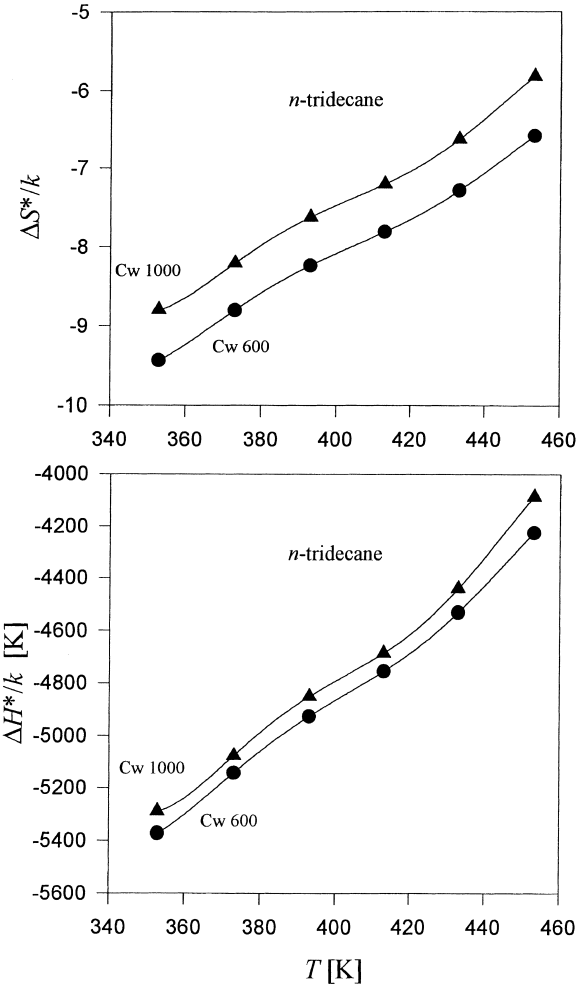

Fig. 8. Variation of enthalpies and entropies of solute transfer with T for *n*-tridecane in Carbowax 600 and 1000. The effect on the alkane solubility is principally due to a variation of entropy for the solute transfer process.

Table 2
Average entropic and enthalpic contributions to the variation Δln K generated by changing the stationary phase from Carbowax 1000 to Carbowax 600

Solute chain length, n	$-\left\langle \frac{\Delta\Delta S^*}{k} \right\rangle$	$-\left\langle \frac{\Delta\Delta H^*}{kT} \right\rangle$	$\frac{\left\langle \Delta\Delta S^*/k \right\rangle}{\left\langle \Delta\Delta H^*/kT \right\rangle}$	Interval of temperature (K)
9	0.536	0.113	4.74	353–413
10	0.566	0.144	3.93	353–413
11	0.575	0.152	3.78	353–413
12	0.596	0.173	3.45	353–413
13	0.616	0.193	3.19	353–453
14	0.651	0.209	3.11	393–453

Increments are defined as $\Delta\Delta S^* = \Delta S^*(\text{CW } 600) - \Delta S^*(\text{CW } 1000)$. The averages are mean values taken in the indicated intervals of temperature.

former stationary phase is softly crosslinked, not presenting important differences with CW 20M, with respect to the values of K [9]. On the contrary, HP-Innowax is densely crosslinked. If we utilize the curve of CW 1000 as a reference in the figure, we can see deep changes in the thermodynamic behavior due to crosslinking. The effect on the shape of the solvation functions is not uniform, as in the case of a simple difference of density (see also Fig. 8).

Measurements for HP-Innowax were made in intervals of 10 °C with the intention of determining the heat capacity difference of solute transfer ΔC_p^*, as was suggested in Ref. [4]. The temperature control in the oven of the employed chromatograph allows the determination of ΔC_p^* only up to 160 °C. At higher temperatures the accuracy of the data was insufficient for this purpose. Only a qualitative approach to the contributions of ΔC_p^* is pretended here. Fig. 10 shows the results for n-dodecane. We can see that there are two overlapped bands. According to Ref. [4], in the chromatographic range the main contributions would arise from motions of the solute's –C–C– backbone. Therefore, at least one of the observed bands should correspond to the bending motions of the solute.

Fig. 11 shows the comparison of isothermal ln $K(n)$ functions for CW 20M [34], AT-wax [9], HP-Innowax, CW 1000 and 600. We see that, resembling an increase in the density of the unmodified PEGs, the effect of increasing the degree of crosslinking consists in a parallel shifting of the curves to lower values of K. We see also that the couple of curves for CW 20M/AT-wax and for CW 1000/HP-Innowax are mutually close, although they have a very different thermodynamic behavior. Obviously, these differences manifest in the temperature dependence of K and not in isotherms such as those of Fig. 11. Another important general aspect concerning this figure is that it is corroborated experimentally that the intercept A of function ln $K(n)$ at $n=1$ is invariably of the same order of ln K of methane [9].

4. Discussion

We shall discuss here solely what seems immediate to the exposed experimental results. We do not intend quantitative theoretical interpretations, due to the requirements of a theoretical framework and unavoidable comparisons with other systems, issues remaining beyond the paper's scope. A theoretical interpretation of these results will be given elsewhere.

We have an ensemble of interrelated experimental facts that concurrently can help us gaining some understand on the solvation phenomena in our system. These may be summarized as follows:

(a) The thermal expansion α_L of PEG is constant in the chromatographic range of T (Fig. 1).

(b) The density ρ_L decreases with the molecular mass of the PEG oligomers (Fig. 2).

(c) The alkane's solubility decreases with the increasing density of the PEG solvent (Fig. 4). This trend is the same as that taking place in a system where the solubility is controlled by the free-volume of the solvent [5]. It must be remarked that the

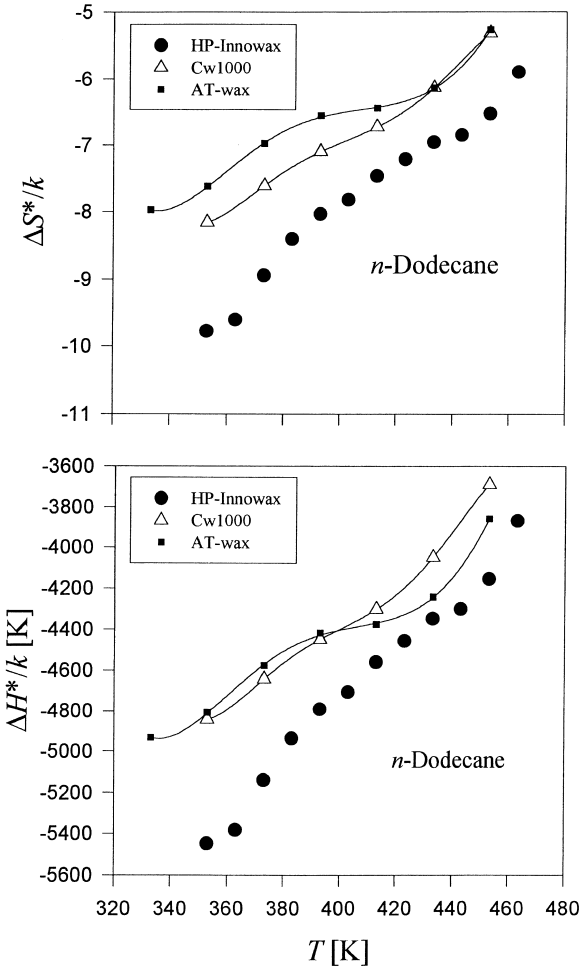

Fig. 9. Variation of enthalpy and entropy with temperature for Carbowax 1000 and the crosslinked phases AT-wax and HP-Innowax.

behavior of the density with the solvent chain length is inverse in Ref. [5], i.e., ρ_L increases with the molecular mass.

(d) Ln K is more simply correlated by the density of molecules than by gravimetric or monomeric densities (Figs. 4–7).

(e) An increment in the solvent density $\Delta\rho$ generates a negative change $\Delta\ln K$ due to an increment of the negative contribution of entropy, $\Delta\Delta S^*$ (Fig. 8). The latter overcomes a small increment of the negative enthalpy $\Delta\Delta H^*$ which contrarily contributes to increase K.

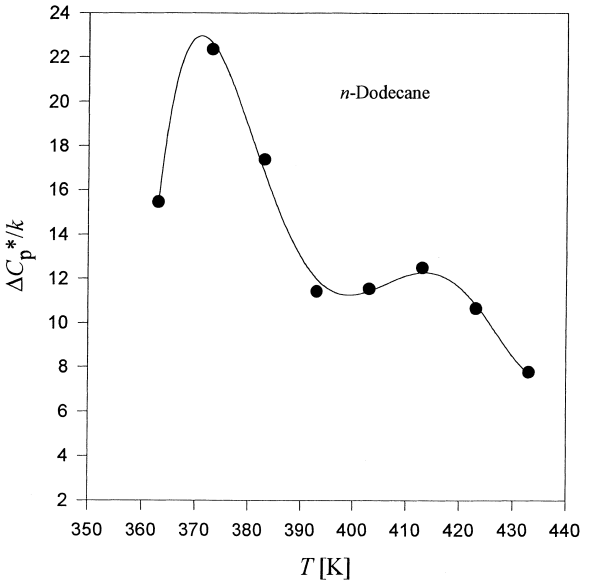

Fig. 10. Behavior with temperature for n-dodecane's heat capacity difference of transfer.

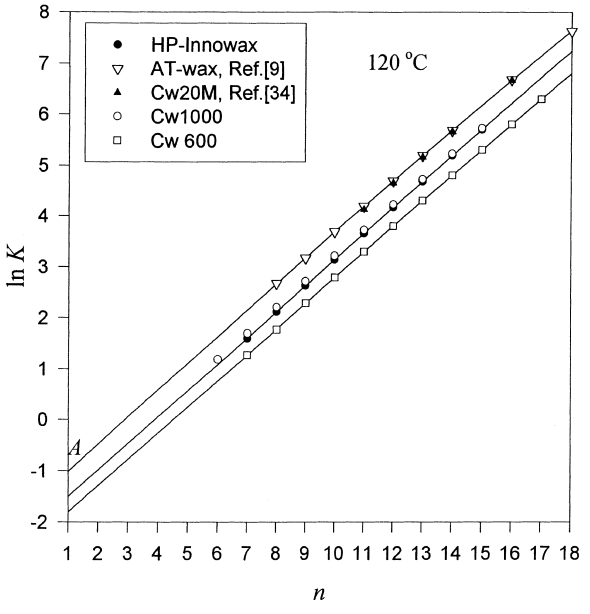

Fig. 11. Variation of ln K with the alkanes carbon number n for different PEG stationary phases at 120 °C. The impact of the free-volume entropy increases as n decreases, therefore, the intercepts A, at $n=1$, reflect that negative contribution to ln K for a hypothetical methylene probe.

(f) The increment $\Delta\Delta S^*$ is weakly dependent on T (Fig. 8).

(g) The impact of $\Delta\Delta S^*$ on $\Delta \ln K$ increases as the solute chain-length n decreases (Table 2).

Point (b) is indicative that the molecular domains of PEG oligomers should be mostly segregated. The reason is that only in such case the pervaded molecular volume grows more steeply ($v_1 \propto n^{\delta}$, $\delta > 2$) than the input of mass ($m_1 \propto n$). In the case of interpenetrated molecular domains, as e.g., poly-(methylene), the density increases with the chain length n. Then point (d) should be expected a priori if $\Delta \ln K/\Delta\rho$ is mainly originated in the effects of excluded volume. This would be consistent with the observation (e). A reduction of the solvent free-volume, V_f, can lead to a decrease of K because it concerns a negative contribution to ΔS^* [4]. According to the (ideal gas/Van der Waals fluid) theoretical partition scheme [31], the free-volume entropy contribution would be given by:

$$\frac{\Delta S_{fv}}{k} = \ln \frac{V_f}{V_L} \tag{5}$$

where V_f is the volume in the dense phase that is accessible to the solute molecule at no energy costs. It depends on the size and shape differences between solute and solvent particles (so, it must not be confused with the total volume of voids in the liquid).

The dependence on T of the free-volume fraction in the liquid, V_f/V_L, is related to the thermal expansion measured by α_L. The free-volume should have a weak dependence on T if no important rearrangements of particles occur within the interval. As stated in point (a), no transitions are observed in the chromatographic range. This is thus consistent with point (f).

According to point (g) and the preceding reasoning, the intercept A of the isotherm $\ln K(n)$ (see Fig. 11) should reflect the free-volume entropic effect, ΔS_{fv}, for a hypothetical isolated methylene probe (which has nearly the same Van der Waals radius of methane). Differences in these intercepts would be mainly originated in variations of the solvent free-volume. The knowledge of A has certain practical chromatographic importance, because it allows the calculation of an unknown phase ratio in a column [8]. This can be done through the least-square regression of $t_R(n)$ data to the retention equation $t_R(n) = t_M + \exp\{[\ln(t_M/\beta) + A] + B(n-1) + \ln(1 - Cn^2)\}$, applicable for $n \geq 5$. Furthermore, being A of the same order of $\ln K$ of methane, it can be utilized for an approximate calculation of the gas hold-up t_M from the retention of methane [8]:

$$t_M = t_R(CH_4) \cdot \frac{\beta}{\beta + e^A} \tag{6}$$

In contrast with ΔS_{fv} of our system, dependent on the volume pervaded by segregated molecules, ΔH^* must depend on the arrangements of small particles around the solute (the radial distribution function) [3]. Apparently, changes of density do not perturb greatly the distribution of monomers surrounding the solute, as Fig. 8 suggests. When restrictions are imposed to the motion of polymer segments, as in crosslinked phases, it is expected a deep change in the distribution of monomers around the solute. The results plotted in Fig. 9 and Fig. 10 suggest that the bending motions of the solute backbone are affected by this change in the solvent force field.

5. Conclusions

Changes in the density of the linear PEG polymer, employed as a stationary phase, affects principally the entropy of transfer for an alkane solute, through the excluded-volume contribution. This limited impact would be the consequence from the fact that the radial distribution function should not undergo important modifications. On the contrary, if the distribution of particles is greatly modified, for example by introducing restrictions to the motion of the polymer segments as in the case of crosslinked phases, deep changes occur to the enthalpy and entropy of transfer. This would be a consequence from the modification of the force field affecting the internal motions of the solute molecule.

Acknowledgements

This work was sponsored by Consejo Superior de Investigaciones Científicas of Spain (CSIC), project PB 98-0537-C02-01. F.R.G. is holder of an external

fellowship from Consejo Nacional de Investigaciones Científicas y Técnicas of Argentina (CONICET) at the Instituto de Química-Física ''Rocasolano'', Madrid, Spain. The authors thank Professor Dr. Carlos Marichal Salinas, from Colegio de México, for his helpful suggestions.

Appendix A

The number-average molecular mass of a polymer is by definition [14]:

$$\bar{M}_n \equiv \frac{\sum_i N_i M_i}{\sum_i N_i} \tag{A.1}$$

N_i is the number of molecules, or moles, that have the molecular mass M_i. The sum is performed overall molecular species i, of different chain lengths, existing in the polymer. Then:

$$\sum_i N_i = \frac{w}{\bar{M}_n} \tag{A.2}$$

where w is the mass of the polymer. If we prepare a polymer blend with components A and B, the total number of moles of the blend will be the sum of the number of moles provided by each component:

$$\sum_i N_i = \sum_A N_A + \sum_B N_B \tag{A.3}$$

By applying Eq. (A.2) to each component and the mixture, and replacing in Eq. (A.3):

$$\frac{w}{\bar{M}_n} = \frac{w_A}{\bar{M}_{nA}} + \frac{w_B}{\bar{M}_{nB}} \tag{A.4}$$

Obviously, the total mass of polymer in the mixture is the sum of those of the components, $w = w_A + w_B$, then:

$$\frac{1}{\bar{M}_n} = \frac{\omega_A}{\bar{M}_{nA}} + \frac{\omega_B}{\bar{M}_{nB}} \tag{A.5}$$

where ω_A and ω_B are the mass fractions of the components. From Eq. (A.5) derives Eq. (1).

The molecular formula of PEG can be written as:

$HO–[CH_2–CH_2–O]_n–H$

Therefore, the relationship between the molecular mass and the degree of polymerization n of a given chain is: $M = 44.05\ n + 18.02$ (g/mole). By applying Eq. (A.1) it can be shown that the number-average degree of polymerization $\bar{n}_n$ is related to $\bar{M}_n$ by:

$$\bar{n}_n = (\bar{M}_n - 18.02)/44.05 \tag{A.6}$$

The third column of Table 1 is calculated in consequence.

According to Eq. (A.2), the number of moles per unit volume of polymer will be:

$$\frac{\sum_i N_i}{V_L} = \frac{w}{V_L \bar{M}_n} = \frac{\rho_L}{\bar{M}_n} \tag{A.7}$$

So the average numeral density of molecules is:

$$\rho_M = \frac{\rho_L N_{Av}}{\bar{M}_n} \tag{A.8}$$

where N_{Av} is Avogadro's number. Usually, ρ_M is expressed in units of nm^{-3}. The average numeral density of monomers is then:

$$\rho_m = \bar{n}_n \rho_M \tag{A.9}$$

Appendix B

The phase ratio of a chromatographic column, at a given temperature T, is by definition:

$$\beta(T) \equiv \frac{V_G(T)}{V_L(T)} = \frac{V_C(T)}{V_L(T)} - 1 \tag{B.1}$$

The second equality, valid only for wall-coated capillaries, states that the internal volume of the column is the sum of the volumes occupied by the gas and liquid phases: $V_C = V_G + V_L$. When the capillary is filled with the coating solution of concentration C_o, at the ambient temperature T_o, the mass of polymer introduced into the column is:

$$w_L = C_o V_C(T_o) \tag{B.2}$$

This is the mass of liquid film that will remain in the column, at any temperature T, once the solvent has been evaporated, then:

$$w_L = \rho_L(T) V_L(T) \tag{B.3}$$

No transitions for the silica material of the column wall take place in the applied range of T. Recalling

the physical notion that a hollow body expands the same as a solid one, the internal volume of the column at T can be calculated using Eq. (2):

$$V_C(T) = V_C(T_o)e^{\alpha_{SiO_2}(T-T_o)} \quad \text{(B.4)}$$

By combining Eqs. (B.2) and (B.4):

$$V_C(T) = \frac{w_L}{C_o}e^{\alpha_{SiO_2}(T-T_o)} \quad \text{(B.5)}$$

By applying Eqs. (B.5) and (B.3) to Eq. (B.1), Eq. (3) is obtained immediately.

References

[1] I. Prigogine, Molecular Theory of Solutions, North Holland, Amsterdam, 1957.
[2] J.H. Vera, J.M. Prausnitz, Chem. Eng. J. 3 (1972) 1.
[3] A. Ben Naim, Solvation Thermodynamics, Plenum Press, New York, 1987.
[4] F.R. González, J. Chromatogr. A 942 (2002) 211.
[5] M.G. Martin, N.D. Zhuravlev, B. Chen, P.W. Carr, J.I. Siepmann, J. Phys. Chem. B 103 (1999) 2977.
[6] P.J. Hesse, R. Battino, P. Scharlin, E. Wilhelm, J. Chem. Eng. Data 41 (1996) 195.
[7] F.R. González, J. Chromatogr. A 832 (1999) 165.
[8] F.R. González, J. Chromatogr. A 873 (2000) 209.
[9] F.R. González, R.C. Castells, A.M. Nardillo, J. Chromatogr. A 927 (2001) 111.
[10] B. Xu, N.P.E. Vermeulen, J. Chromatogr. 445 (1988) 1.
[11] J.K.G. Kramer, R.C. Fouchard, K.J. Jenkins, J. Chromatogr. Sci. 23 (1985) 54.
[12] V.G. Berezkin, A.A. Korolev, Chromatographia 20 (1985) 482.
[13] P. Sandra, F. David, R.A. Turner, H.M. Mc Nair, A.D. Brownstein, J. Chromatogr. 411 (1989) 63.
[14] W. Peebles, Molecular Weight Distributions in Polymers, Academic Press, New York, 1968.
[15] O. Schweitzer, H. Staudinger, Chemische Berrichte 62 (1929) 2395.
[16] H. Staudinger, From Organic Chemistry to Macromolecules, Wiley-Interscience, New York, 1970.
[17] S.R. Sandler, W. Karo, Polymer Synthesis, Vols. I and III, Academic Press, New York, 1974.
[18] H.G. Elias, Macromolecules, 2nd ed., Synthesis, Materials and Technology, Vol. 2, Plenum Press, New York, 1984.
[19] F.E. Bailey, J.V. Koleske, Polyethylene Oxide, Academic Press, New York, 1976.
[20] D.K. Thomas, A. Charlesby, J. Polym. Sci. 42 (1960) 195.
[21] F.N. Hill, F.E. Bailey, J.T. Fitzpatrick, Ind. Eng. Chem. 50 (1958) 5.
[22] R.A. Miller, C.C. Price, J. Polym. Sci. 34 (1959) 161.
[23] D.O. Hummel, IR Spectra of Polymers in the Medium and Long Wavelength Regions, Wiley, New York, 1966.
[24] S.A. Taleb-Bendiab, J.M. Vergnaud, J. Chromatogr. 107 (1975) 15.
[25] J. Klein, J.E. Jeberien, Makromol. Chem. 181 (1980) 1237.
[26] M.B. Evans, J.F. Smith, J. Chromatogr. 36 (1968) 489.
[27] F.W. Billmeyer, Textbook of Polymer Science, 3rd ed., Wiley-Interscience, New York, 1984.
[28] D.F. Fritz, E. Kovats, Anal. Chem. 45 (1973) 1175.
[29] D.E. Martire, Anal. Chem. 46 (1974) 626.
[30] HyperChem, Computational Chemistry, Hypercube, Ontario, 1996.
[31] F.R. González, J.L. Alessandrini, A.M. Nardillo, J. Chromatogr. A 852 (1999) 583.
[32] B.R. Kersten, S.K. Poole, C.F. Poole, J. Chromatogr. 468 (1989) 235.
[33] K. Grob, Making and Manipulating Capillary Columns for Gas Chromatography, Hüthig, Heidelberg, 1986.
[34] C.F. Poole, Q. Li, W. Kiridena, W.W. Koziol, J. Chromatogr. A 898 (2000) 211.
[35] B.R. Kersten, C.F. Poole, J. Chromatogr. 399 (1987) 1.
[36] C.F. Poole, T.O. Kollie, S.K. Poole, Chromatographia 34 (1992) 281.
[37] V.G. Berezkin, Adv. Chromatogr. 40 (2000) 599.